Applied Chemistry Today **20(77)** (2025) 11-22

Semnan University

Applied Chemistry Today

Journal homepage: https://chemistry.semnan.ac.ir/

ISSN: 2981-2437

Research Article

Photocatalytic Oxidation of Benzyl Alcohol to Benzaldehyde over Visible Light Sensitized n-TiO_2-P25 as Photocatalyst

Mehrnoosh Bitaraf, Ali Amoozadeh * and Mahdi Asghari

Department of Organic Chemistry, Faculty of Chemistry, Semnan University, Semnan, Iran

PAPER INFO

Article history:
Received: 26/Dec/2024
Revised: 09/Feb/2025
Accepted: 08/Mar/2025

Keywords:
TiO_2-P25,
Photo-oxidation,
Photocatalyst,
Sensitization,
Visible light,
Plant dye,
Henna

ABSTRACT

In the present work, henna plant dye was used as a natural photo-sensitizer for n-TiO_2-P25 semiconductor. The prepared sensitized nano-photocatalyst was then properly used to selectively oxidize benzyl alcohol to benzaldehyde. The henna natural dye has shown appreciable adsorption onto the surface of n-TiO_2-P25 and forms an organic-inorganic composite. The obtained composite improved the photochemical and photocatalytic properties of nano-titanium dioxide semiconductor. The characteristics of the henna sensitized n-TiO_2-P25 were investigated through convenient analyses such as Fourier transform infrared spectroscopy (FTIR), thermogravimetric analysis (TGA), Field emission scanning electron microscopy (FE-SEM), Transmission electron microscopy (TEM), X-Ray Diffraction (XRD), and UV-visible/DRS techniques. According to these analyses, the as-prepared composite reduced the band gap energy of titanium dioxide nano-particles and led to the response to visible light. Under the blue LED light irradiation, henna sensitized n-TiO_2-P25 oxidized benzyl alcohol to benzaldehyde with excellent selectivity, high yield and short reaction times. Applying henna natural dye as a photo-sensitizer is a more convenient, more cost-effective and greener approach, in comparison with the toxic and costly synthetic dyes.

DOI: https://doi.org/10.22075/chem.2025.36342.2328

* **.Corresponding author:** Professor of Organic Chemistry. *E-mail address: aamozadeh@semnan.ac.ir*

How to cite this article: Bitaraf, M., Amoozadeh, A., & Asghari, M. (2025). Photocatalytic Oxidation of Benzyl Alcohol to Benzaldehyde over Visible Light Sensitized n-TiO_2-P25 as Photocatalyst. *Applied Chemistry Today*, **20(77)**, 11-22. (in Persian)

1. Introduction

Selective photo-oxidation reactions of aromatic alcohols into their corresponding aldehydes has been at the core of many academic research studies due to their importance [1-3]. Aldehyde derivatives are important precursors for various industries. Titanium dioxide (TiO_2) is the best candidate to catalyze photo-oxidation reactions. TiO_2 is a promising photocatalyst semiconductor with outstanding properties such as non-toxicity, abundance, and cost-effectiveness [4-7]. Commercial TiO_2-P25 or Degussa P25 is a mixture of rutile and anatase phases of TiO_2 (30:70) that has gained significant attention from researchers [8-11]. TiO_2-P25 has shown photocatalytic activity upon exposure to UV illumination, mercury lamp, or sunlight[12]. However, its wide band gap, however, has restricted the application of TiO_2-P25 photocatalyst as its activation is achieved only by the ultraviolet irradiation. Consequently, modification methods are needed for TiO_2 to respond to visible light. These methods are called surface sensitization [13-15]. The main role of a sensitizer is to sensitize the surface of the semiconductor to visible light. In fact, visible light excites an electron from sensitizer, and thus, the excited electron transfers to the semiconductor. Organic dyes, metal complexes, and polymers have been used conveniently as sensitizers [16-18]. In dye sensitization, dye molecules are physically adsorbed on the semiconductor surface to form an organic-inorganic composite. As a result, the light harvesting capacity of the photocatalyst improves. Organic dyes and natural dyes extracted from plants have also been studied to explore their application as photosensitizer. According to reports, organic dyes have worked efficiently. However, these dyes have complicated synthetic processes and high cost. On the other hand, the natural dyes from different parts of plants are more available and cost-effective. Non-toxicity and biodegradability are other advantages of natural dyes [19-21].

Henna (Lawsonia Inermis) is one of the plant-based natural dyes that has been used for dyeing hair and skin since ancient times. The main active component in henna leaves is lawsone (2-hydroxy-1,4-naphthoquinone)[22]. It is an orange pigment with conjugated bonds. The availability, compatibility and non-toxicity of henna encouraged us to investigate its possibility as photosensitizer on TiO_2-P25 nanoparticles. This molecule can easily adsorb onto n-TiO_2-P25 due to the condensation of hydroxyl protons with surface hydroxyl groups of n-TiO_2. Accordingly, henna sensitized n-TiO_2-P25 was prepared and employed as a photocatalyst for the photo-oxidation reaction of benzyl alcohol to benzaldehyde.

2. Result and Discussion

In this study, we have rationally designed a green and cost-effective strategy to sensitize the nano-TiO_2-P25 photocatalyst by using henna plant dye. Characterization of the sensitized nano-photocatalyst was accomplished through convenient methods.

2.1. Thermogravimetric analysis

Thermogravimetric analysis (TGA) analysis is a useful tool to assess the chemisorption and thermal stability of modified nanoparticles. In this regard, TGA analysis of sensitized n-TiO_2-P25 with three different concentrations of henna (1, 3, and 5 mg/ l) was carried out from 25 to 600 ^oC to evaluate the adsorption of the organic components to the surface of n-TiO_2-P25. From figure 1, it is clear that all three nanoparticles have the same weight loss pattern; a weight loss step below 100^oC and the next step from 100 to 400^oC. These steps of weight loss are related to the complete collapse of henna. The maximum thermal stability of the as-prepared nanoparticle is up to 400^oC. It can be seen that the nanoparticle functionalized with the 3 mg/l (Fig. 1b)

shows the highest weight loss. For n-TiO_2-P25 functionalized with 5mg/l henna (Fig. 1c), it seems that the surface was saturated, and thus, the weight loss (loading amount) in diagram c is smaller than for diagram b. The rest of the analysis was performed on nanoparticle with highest amount of loading.

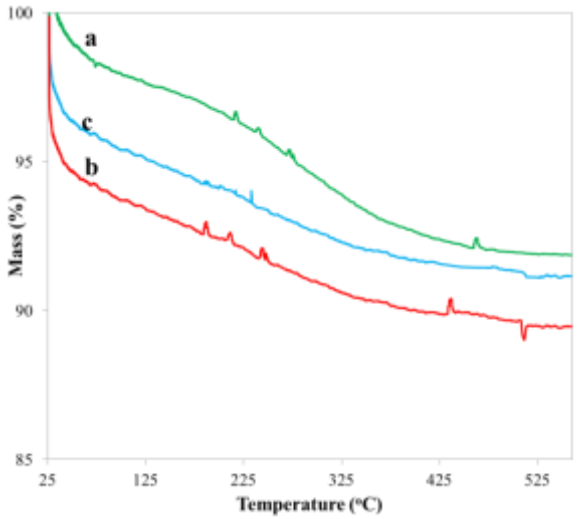

Fig. 1. TGA curves of n-TiO_2-P25 sensitized with a) 1mg/L, b) 3mg/L, and c) 5mg/L henna.

2.2. Fourier transforms infrared spectroscopy

Fourier transform infrared (FT-IR) spectroscopy has been regarded as one of the best methods to study the presence of functional groups on nanoparticles. In this regard, n-TiO_2-P25 was explored before and after the sensitization procedure. As shown in figure 2a, the FTIR results of bare n-TiO_2-P25 presents distinguished peaks at 1620 and 3355 cm^{-1} which is assigned to the surface hydroxyl groups. The broad absorption band in wavenumbers below 900 cm^{-1} is indicative of Ti-O-Ti bond vibrations. Figure 2b, shows henna sensitized n-TiO_2-P25 with the exact pattern of n-TiO_2-P25 along with weak vibrations of characteristic functionalities of lawsone. Surface hydroxyl groups of TiO_2 appear at 1623 cm^{-1} alongside C=O stretching at 1647 cm^{-1}. Additionally, C=C vibrations of the ring are visible at 1419 and 1458 cm^{-1}. Stretching vibration of H-bonded hydroxyl of phenol is covered by the hydroxyl band at 3400 cm^{-1}. Weak vibrational bands of lawsone indicate that a small amount of henna is physically adsorbed on the surface of n-TiO_2-P25, consistent with the data from TGA.

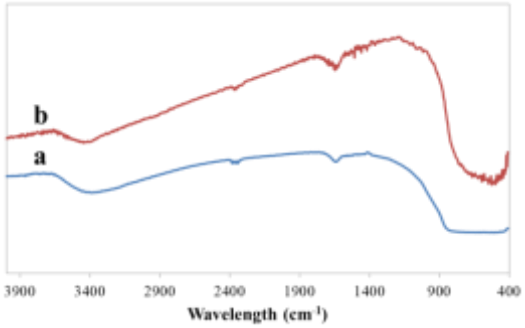

Fig. 2. The FT-IR spectra of a) bare n-TiO_2-P25 and b) henna sensitized n-TiO_2-P25.

2.3. X-Ray Diffraction analysis

X-Ray Diffraction analysis (XRD) was performed to determine the exact crystal structure of the prepared organic-inorganic composite. Bare n-TiO_2-P25 consists of both of anatase and rutile phases. As shown in figure 3a, the crystallogram of n-TiO_2-P25 shows the main diffractive peaks at 25.31° [for anatase (101)] and 27.411° [for rutile (110)], as characteristic lines[23]. Figure 3b, shows the pattern of henna sensitized n-TiO_2-P25, indicating that the presence of an organic moiety does not change the crystal structure.

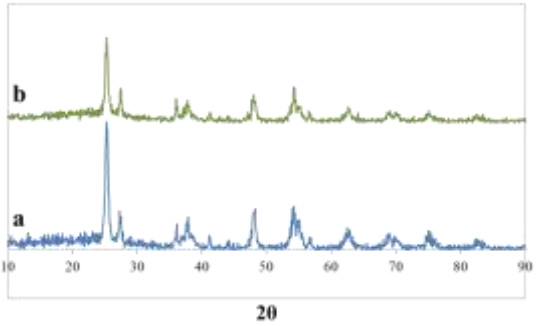

Fig. 3. XRD patterns of a) n-TiO_2-P25, and b) Henna sensitized n-TiO_2-P25.

2.4. Morphology analysis

Field emission scanning electron microscopy (FE-SEM) was used to visualize size and surface morphological details of nanoparticles as shown in

Figure 4. TiO_2-P25 nano-particles show an approximate diameter of 28.55-42.54 nm with nearly spherical shapes (Figure 4a) which are distributed uniformly. The final henna sensitized n-TiO_2-P25 particles are still morphologically spherical with a larger size of 30–70 nm (Figure 4b). These results prove the presence of the sensitized photocatalyst in nanometer-sized particles.

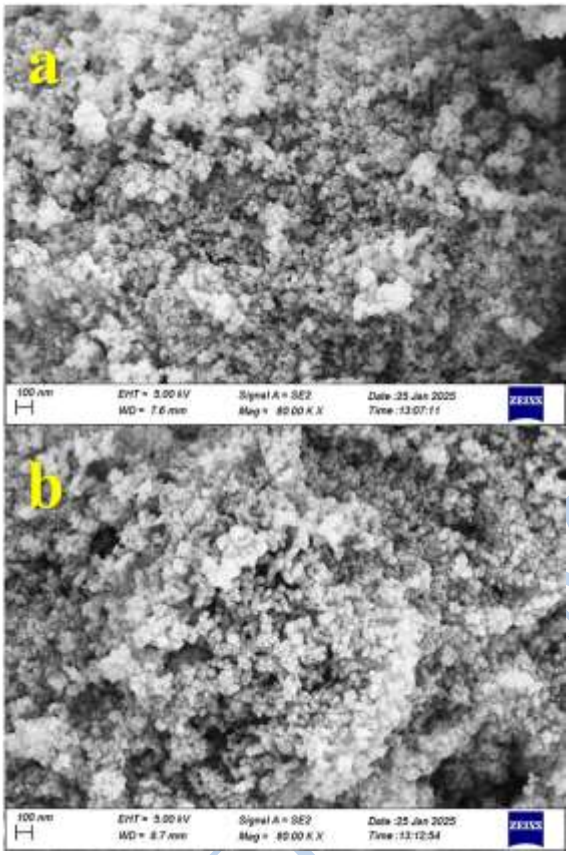

Fig. 4. FE-SEM images of a) bare n-TiO_2-P25 and b) henna sensitized n-TiO_2-P25.

In order to further survey the type and content of the elements on the nano-photocatalyst, Energy dispersive X-ray spectroscopy (EDX) was performed. The results are given in figure 5. There are three elements; Ti, O, and C in the sensitized photocatalyst; O and Ti have the highest contents, as expected, and C the lowest. The content of C reflects the amount of loaded organic dye on the surface of nanoparticles (along with a part of O). Accordingly, the relatively low content of carbon, shows the low adsorption of henna on the surface which is in agreement with TG analysis.

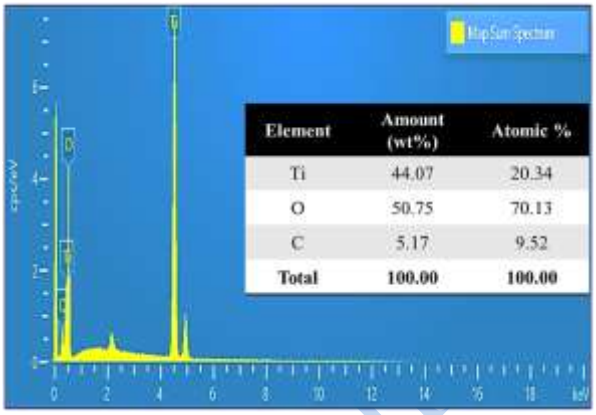

Fig. 5. EDX spectrum of henna sensitized n-TiO_2-P25 (illustrated as element type and content analysis).

To further investigate the elemental composition and distribution in the prepared nano-photocatalyst, the EDX-mapping analysis was carried out (Figure 6). The map images also affirm the presence of C element that represents adsorbed organic moiety (henna dye) that is homogeneously distributed on the surface of henna sensitized n-TiO_2-P25. The map of Ti and O elements, represented by red and green colors respectively, indicate the main structure of the substrate, n-TiO_2-P25.

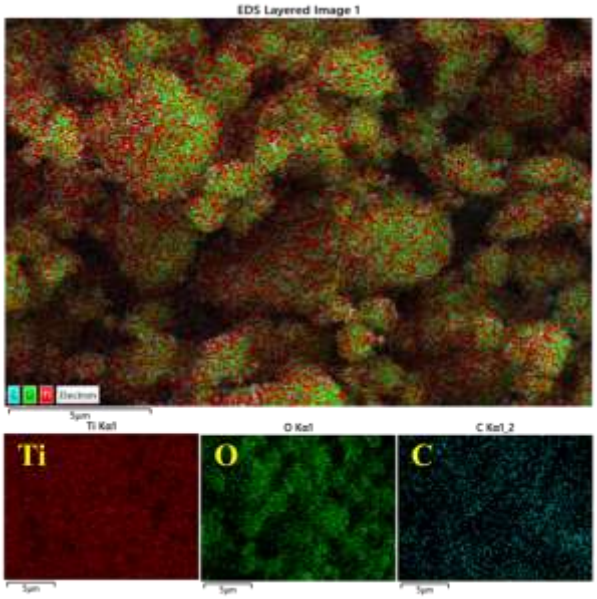

Fig. 6. Elemental mapping analysis of henna sensitized n-TiO_2-P25.

Figure 7 displays Transmission Electron Microscopy (TEM) images of henna sensitized n-TiO_2-P25 that confirms the spherical and nanosized particles of the as-prepared photocatalyst (in agreement with FE-SEM images). Because the dye molecules are organic and have low electronic density, the image shows only n-TiO_2-P25 particles. The dark spots indicate the aggregation of the nano-particles.

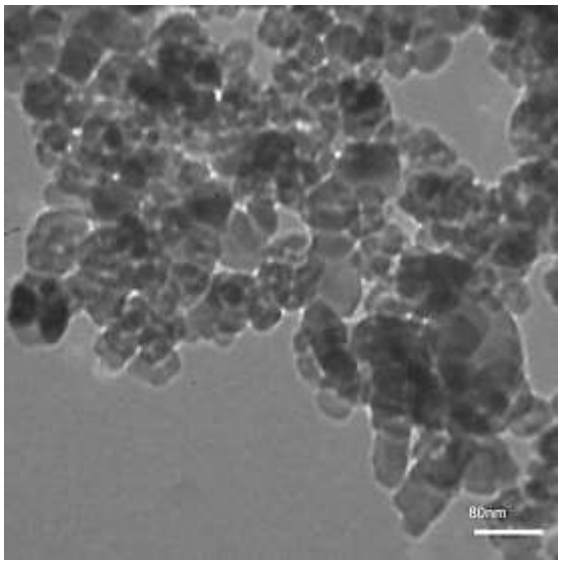

Fig. 7. TEM images of henna sensitized n-TiO_2-P25.

2.5. Adsorption experiments

The adsorption-desorption process of dye on the surface of titanium dioxide can be described using adsorption isotherms. Adsorption isotherms describe the relation between the amount of adsorbate (dye) on the adsorbent surface and its concentration in solution at equilibrium. Two most common isotherm models are Langmuir isotherm and Freundlich isotherm. The Langmuir isotherm express that the adsorption on the adsorbent surface is monolayer (equation 1).

$$q_e = (q_{max} KC_e)/(1+KC_e) \quad (1)$$

Where q_e is the amount of adsorbate per unit mass of adsorbent, q_{max} is the maximum adsorption capacity, K is Langmuir constant, and C_e is the equilibrium concentration of adsorbate. The Freundlich isotherm express that the adsorption on the adsorbent surface is not monolayer and varies across the surface (equation 2).

$$q_e = KC_e^{1/n} \quad (2)$$

Where n is adsorption intensity constant. To determine the isotherm experimentally, the process involves measuring the equilibrium adsorption capacity (q_e) of the dye with different initial concentrations (C_0= 1, 5, 15, 25, 50 ppm). In the next steps, an accurate amount of nano-titanium dioxide (0.01 g) was added to a known volume (V= 50 ml) of each dye (henna) solution. The obtained mixtures were placed in ultrasonic bath. After an appropriate time, n-TiO2-P25 was separated using centrifuge, and the concentration of the henna solutions was measured using UV-Vis spectrophotometry. The adsorption capacity (q_e) was calculated for each solution using the following equation:

$$q_e = (C_0-C_e).V/m \quad (3)$$

Here, V is the volume of the solution of adsorbate, and m is the mass of adsorbent. Then, the adsorption capacity (q_e) was plotted versus the equilibrium concentration (C_e). The obtained plot (figure 8) was well fitted to linear Langmuir isotherm model to extract the maximum adsorption capacity (q_{max}) which indicates the maximum amounts of henna dye that can be adsorbed per unit mass (g) of n-TiO_2-P25. The linear equation, after removing outliers is as indicated at figure 8:

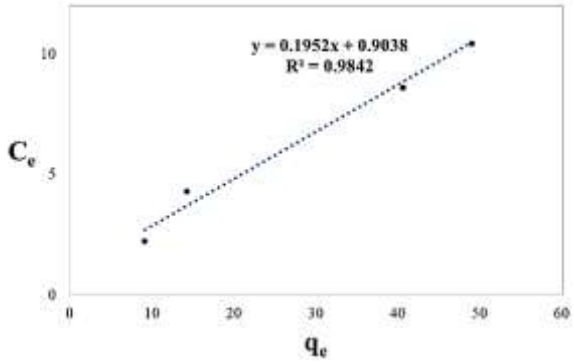

Fig. 8. Equilibrium data on the adsorption of henna dye on n-TiO2-P25 particles.

And the maximum adsorption capacity was determined 5.123 mg per g of n-TiO_2-P25 from the slope of the linear equation.

These data revealed that the adsorption of henna on n-TiO_2-P25 occurs through a monolayer process, and titanium dioxide under these conditions, did not exhibit significant adsorption capacity for henna dye. This is fully consistent with the data obtained from TG analysis. Nevertheless, as a sensitized photocatalyst, it was able to efficiently carry out the photocatalytic oxidation of benzyl alcohol to benzaldehyde.

Zeta (ζ) potential is a measure of the electrostatic potential at the surface of a particle. It reflects the charge distribution around the particle (nano-particle), which influences how particles interact with each other and with other species. Zeta potential was determined for n-TiO_2-P25 before and after sensitization with henna and the result is depicted in figure 9. According to the results, the negative charge of the TiO_2-P25 nanoparticles (z = -28.8 mV) was decreased (z = -14.7 mV) upon the addition of henna dye, confirming the interaction (and adsorption) of the henna onto the TiO_2 NPs (Fig. 9). This interaction has led to the partial adsorption of henna onto the surface of titanium dioxide.

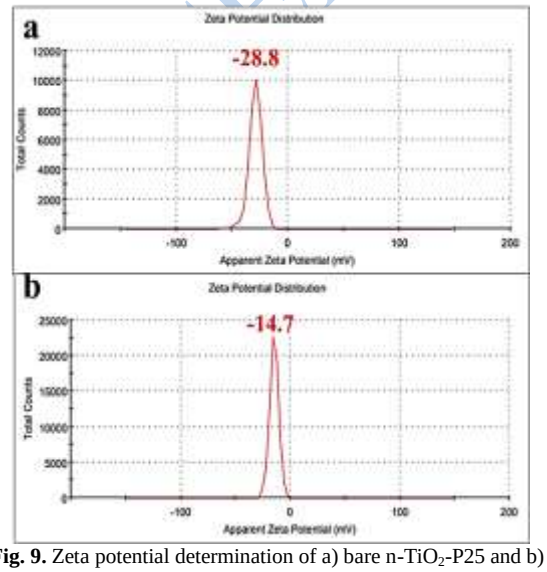

Fig. 9. Zeta potential determination of a) bare n-TiO_2-P25 and b) henna sensitized n-TiO_2-P25.

2.6. UV-Visible/DRS analysis

The optical properties of the obtained nano-photocatalysts were determined through UV-visible/DRS spectral data. The UV-visible absorption spectrum for each nanoparticle is shown in figure 10. Both nanoparticles indicate broad and strong absorptions in the UV region. As shown in Fig. 10(a), n-TiO_2-P25 has a strong absorption at 325 nm. For henna sensitized n-TiO_2-P25, in Fig. 10(b), although the maximum absorption is at 340 nm, the absorption edge has a slight redshift of ≈15 nm in comparison with bare TiO_2-P25 nanoparticles. This result shows that the sensitization extended the absorption edge of n-TiO_2-P25 toward the visible region which makes a relative blue-light response for the obtained photocatalyst.

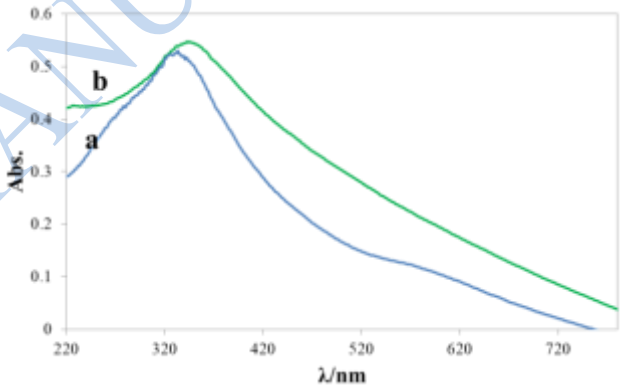

Fig. 10. UV-Visible absorption spectra of a) bare n-TiO_2-P25 and b) henna sensitized n-TiO_2-P25.

Diffuse reflectance spectroscopy (DRS) was also performed on bare and sensitized nTiO_2-P25. As can be seen in figure 11, the band gap energy of the sensitized photocatalyst (2.92 eV) showed an acceptable reduce in comparison with the bare n-TiO_2-P25 (3.13 eV); resulting in a slight redshift. Thus, the photoactivity of the sensitized n-TiO_2-P25 was improved.

2.7. Photocatalytic activity study

To investigate the photocatalytic activity of the sensitized photocatalyst, a series of experiments were conducted under visible light (blue LED, λ > 420 nm) irradiation.

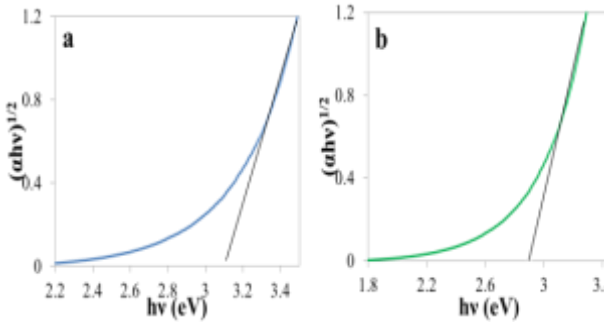

Fig. 11. Kubelka–Munk energy curve plots of a) bare n-TiO_2-P25 and b) henna sensitized n-TiO_2-P25.

The results of optimization steps are summarized in Table 1. First, a solution of benzyl alcohol in acetonitrile was exposed to the sensitized nanoparticle in the presence of $NaNO_3$ as an appropriate oxidant, in the dark (Table 1, entry 1). No progress was observed which indicated the photocatalytic role of the nanoparticle. Then, 0.01 g sensitized n-TiO_2-P25 was employed to catalyze the reaction of 0.1 mmol benzyl alcohol and 0.1 mmol $NaNO_3$ in 5 mL acetonitrile, which are the optimum conditions. Under 4 × 3 W blue LED light irradiation, the sensitized photocatalyst completed the reaction in 3 hours with 70% yield and 100% selectivity (Table 1, entry 3).

Table 1. The optimization of reaction conditions for oxidation of benzyl alcohol[a]

Entry	Catalyst amount (g)	Light source	Reactant amount (mmol)	Oxidant amount (mmol)	Yield[b] /Selectivity (%)
1	0.01	dark	0.01	0.01	-
2	0.005	Blue LED	0.01	0.01	30/>99
3	0.01	Blue LED	0.01	0.01	70/>99
4	0.03	Blue LED	0.01	0.01	30/>99
5	0.01	Blue LED	0.005	0.01	50/>99
6	0.01	Blue LED	0.03	0.01	55/>99
7	0.01	Blue LED	0.01	0.005	30/>99
8	0.01	Blue LED	0.01	0.03	50/>99

[a] Solvent: acetonitrile; light source: 4 × 3 W blue LED; room temperature, and time: 3 hours.

[b] Yield was determined by UV-visible spectroscopy.

The time-course diagram for the photo-oxidation of benzyl alcohol in the presence of sensitized n-TiO_2-P25 photocatalyst under the optimized conditions is shown in figure 12. It shows that after 3 hours, no progress was observed and apparently the reaction stopped with 70% yield and 100% selectivity.

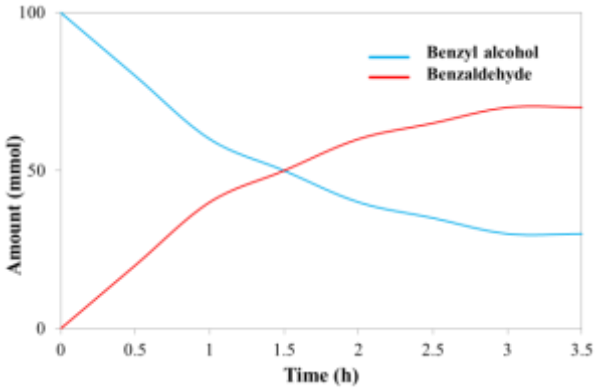

Fig. 12. Experimental results of oxidation of benzyl alcohol by henna sensitized n-TiO_2-P25 under blue light irradiation.

A comparison between bare n-TiO_2-P25 and the sensitized photocatalyst for oxidation of benzyl alcohol under optimized condition is conducted and demonstrated in Table 2. Clearly, the henna sensitized nanoparticle showed increased photocatalytic activity under blue light irradiation.

Table 2. Comparison of reaction efficiency for different catalytic systems under the optimized conditions[c]

Entry	catalyst	Yield[d] /Selectivity (%)	Time (h)
1	Bare n-TiO_2-P25	-	3
2	Henna sensitized n-TiO_2-P25	70/>99	3

2.8. Possible mechanism

A possible mechanism is proposed for photocatalytic oxidation of benzyl alcohol to benzaldehyde, based on the literature[24-26]. Under visible light irradiation, the henna dye adsorbed on the surface of n-TiO_2-P25 is excited to dye*,

[c] Solvent: acetonitrile; light source: 4 × 3 W blue LED and room temperature.

[d] Yield was determined by UV-visible spectroscopy.

resulting in injection of an electron to the conduction band (CB) of TiO_2-P25. The migration of electrons generates a dye radical cation, $dye^{\cdot+}$. Benzyl alcohol reacts to the $dye^{\cdot+}$ to form benzyl alcohol radical and H^+, and $dye^{\cdot+}$ returns to its ground state. On the other side, electrons on conduction band reduce the nitrate ion as describe in one of the equations below:

$$NO_3^- + 2e^- + 2H^+ \rightarrow NO_2^- + H_2O \quad (4)$$

$$NO_3^- + 8e^- + 9H^+ \rightarrow NH_3 + 3H_2O \quad (5)$$

$$NO_3^- + 10e^- + 12H^+ \rightarrow N_2 + 6H_2O \quad (6)$$

According to the literature[27-29], and considering equations 4-6, the stoichiometric ratio of H^+ to nitrate ion determines the ultimate product of the reduction. The higher the ratio, the more efficient the reduction. This is why the presence of a Brønsted acid improves the photochemical yield. In this work, in the absence of Brønsted acid, the required H^+ comes from the oxidation of benzyl alcohol according to the following equation:

$$BnOH \rightarrow PhCHO + e^- + H^+ \quad (7)$$

We think that the produced amount of H^+ from equation 7 is not sufficient to completely reduce nitrate and at best, nitrate is reduced to nitrite.

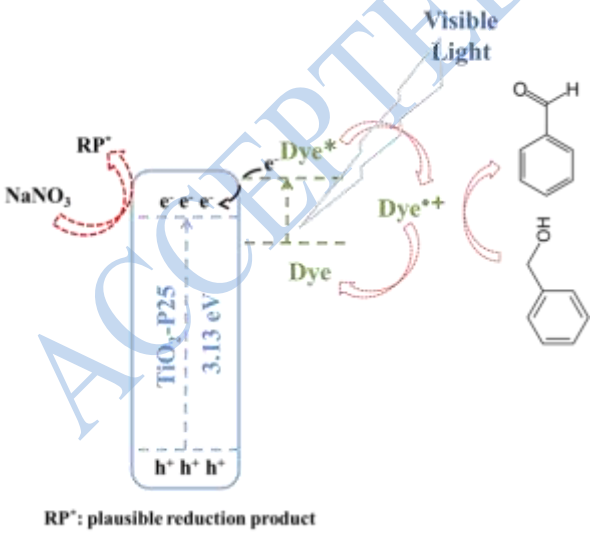

Fig. 13. Possible mechanism of oxidation of benzyl alcohol to benzaldehyde over henna sensitized n-TiO_2-P25 photocatalyst.

3. Experimental section

All chemicals used were of commercial reagent grade and supplied by Aldrich and Merck. TiO_2-P25 (ca. 70% anatase, 30% rutile) nano powder was supplied by Degussa Co. The purity of the synthesized compounds and progress of reactions was assayed by Shimadzu UV-Visible 1650 PC spectrophotometer in the range of 200–800 nm using a quartz cell with an optical path of 1 cm. Fourier transform infrared spectroscopy (FT-IR) was conducted on a Shimadzu FT-IR 8400 equipment using KBr pressed powder plates in the range of 400–4000 cm^{-1}. Thermogravimetric analyses (TGA) were performed on a Du Pont 2000 thermal analysis apparatus under air atmosphere heated from 25 °C to 600 °C at a ramp rate of 5 °C per minute. The optical band gap (Eg) of TiO_2-P25 nanoparticles before and after sensitization was determined by Diffuse Reflectance Spectroscopy (DRS, Model Sinco S4100, Korea). X-ray diffraction (XRD) measurement was carried out on a Siemens D5000 diffractometer with Cu-Kα radiation of wavelength 1.54 Å. Field emission scanning electron microscope (FESEM) images and energy dispersive X-ray (EDX) spectra were executed on a Sigma 300-HV scanning electron microscope instrument operating at 10 kV. Transmission electron microscopy (TEM) was obtained with a Philips EM208S, 100KV TEM digital transmission microscope.

3.1. Sensitization of n-TiO_2-P25 with henna

Henna sensitized n-TiO_2-P25 was prepared as follows. In a typical procedure, a 50 mL solution of henna with concentrations of 1, 3, and 5 mg/L was prepared. Then, 0.01 g TiO_2-P25 was added to each solution and sonicated for an hour. The ultimate functionalized nanoparticle was then centrifuged and dried at 80°C for 24 hours.

3.2. Photocatalytic reaction

The photo-catalytic performance of the sensitized n-TiO_2-P25 was tested via the oxidation reaction of benzyl alcohol[8]. The photo-oxidation of benzyl alcohol was performed in a 10 mL Pyrex round-

bottom flask, in which the henna sensitized n-TiO_2-P25 (0.01 g) was suspended in a solution of benzyl alcohol (0.01 mmol) in acetonitrile (5 mL). Selective photo-oxidation of alcohols to their corresponding aldehydes is always carried out in organic solvents such as benzontrifluoride or acetonitrile. Also, sodium nitrate salt (0.01 mmol) was added to the suspension as the oxidant and the obtained mixture was magnetically stirred. The reactions were performed at ambient temperature using blue LED lamps (4×3W) with a wavelength range of $\lambda > 420$ nm.

At predetermined times, sample aliquots were taken from the reaction mixture and then photocatalytic nanoparticles were removed by centrifugation. Yield and selectivity of the product were monitored by UV−Vis spectroscopy (at the maximum wavelength of benzaldehyde in acetonitrile at 241 nm).

4. Conclusions

Henna natural dye was used as a photosensitizer and the properties of the resultant photocatalyst were characterized appropriately. The henna sensitized nano-photocatalyst showed a good redshift, leading to a better performance in the visible region. The improved optical properties of n-TiO_2-P25 after sensitization are attributed to forming an organic-inorganic composite. In these composites, the dye reaches the excited state after exposure to visible light. Then, electrons are injected from the excited state of the dye to the CB of the inorganic semiconductor (TiO_2-P25). The injected electrons travel to the surface of the inorganic semiconductor and react with oxidant whereas the formed holes react with the organic reagents. The presented sensitization method is practicable for different kinds of plant based dyes. In comparison with synthetic dyes, this approach is more convenient and more cost-effective. Besides, using plant based dyes as photosensitizer is a more green, safe, and environmental friendly approach. The prepared nanoparticles were capable of conveniently catalyze the photo-oxidation of benzyl alcohol with good yields and high selectivity, in short times.

Acknowledgments This research is supported by the Postdoc grant of the Semnan University (number 31129). Also, the authors wish to thank the faculty of chemistry of Semnan University.

Conlicts of Interest

The author declares that there is no conflict of interest regarding the publication of this manuscript. In addition, the authors have entirely observed the ethical issues, including plagiarism, informed consent, misconduct, data fabrication

References

[1] Hosseini, S.;Amoozadeh, A.;Akbarzadeh, Y. (2019). Nano-WO3-SO3H as a New Photocatalyst Insight Through Covalently Grafted Brønsted Acid: Highly Efficient Selective Oxidation of Benzyl Alcohols to Aldehydes. *Photochemistry and photobiology*. *6* (95), 1320-1330.

[2] Ye, X.;Chen, Y.;Wu, Y.;Zhang, X.;Wang, X.;Chen, S. (2019). Constructing a system for effective utilization of photogenerated electrons and holes: Photocatalytic selective transformation of aromatic alcohols to aromatic aldehydes and hydrogen evolution over Zn3In2S6 photocatalysts. *Applied Catalysis B: Environmental*. (242), 302-311.

[3] Unsworth, C.A.;Coulson, B.;Chechik, V.;Douthwaite, R.E. (2017). Aerobic oxidation of benzyl alcohols to benzaldehydes using monoclinic bismuth vanadate nanoparticles under visible light irradiation: Photocatalysis selectivity and inhibition. *Journal of catalysis*. (354), 152-159.

[4] Guo, W.;Guo, T.;Zhang, Y.;Yin, L.;Dai, Y. (2023). Progress on simultaneous photocatalytic degradation of pollutants and production of clean energy: A review. *Chemosphere*. (339), 139486.

[5] Ali, S.;Abdul Nasir, J.;Nasir Dara, R.;Rehman, Z. (2022). Modification strategies of metal oxide photocatalysts for clean energy and environmental applications: A review. *Inorganic Chemistry Communications*. (145), 110011.

[6] Piroozi, S.;Tanhaei, B.;Ayati, A.;Niknam Shahrak, M.;Saei Moghadam, M. (2022). Investigation of photo catalytic properties of ZIF-8 emitted based on titanium dioxide nano tubes in removal of aqueous pollutants. *Applied Chemistry Today*. *62* (17), 99-114.

[7] Khalil, M.;Kadja, G.T.M.;Ilmi, M.M. (2021). Advanced nanomaterials for catalysis: Current progress in fine chemical synthesis, hydrocarbon processing, and renewable energy. *Journal of Industrial and Engineering Chemistry*. (93), 78-100.

[8] Amini, Z.;Givianrad, M.H.;Aberoomand Azar, P.;Husain, S.W.;Saber Tehrani, M. (2020). Photocatalytic and photoelectrocatalytic degradation of congo red dye using Cu and S co-doped TiO2/SiO2 nanoparticles under the purple LED light irradiation: optimization of operational conditions. *Applied Chemistry Today*. *54* (15), 299-314.

[9] Bitaraf, M.;Amoozadeh, A. (2021). The first report of covalently grafted semiconductors; n-TiO2-P25@ECH@WO3 as a new, efficient, robust and visible-light-responsive photocatalyst. *Journal of Chemical Technology & Biotechnology*. *4* (96), 963-970.

[10] Bitaraf, M.;Amoozadeh, A. (2021). A novel sery of SO3H-functionalized heterostructure nano-semiconductors; an efficient strategy to prepare visible-light responsive photocatalysts. *Res Chem Intermed*. *8* (47), 3329-3347.

[11] López, J.;Rey, A.;Viñuelas-Zahinos, E.;Álvarez, P.M. (2023). Preparation of a new green magnetic Fe3O4 @TiO2-P25 photocatalyst for solar advanced oxidation processes in water. *Journal of Environmental Chemical Engineering*. *3* (11), 109999.

[12] Taghavi, S.;Amoozadeh, A.;Nemati, F. (2021). The first report of deep eutectic solvent (DES) nano-photocatalyst (n-TiO2-P25@TDI@DES (urea: ZnCl2)) and its application on selective oxidation of benzyl alcohols to benzaldehydes. *Journal of Chemical Technology & Biotechnology*. *2* (96), 384-393.

[13] Guo, Q.;Zhou, C.;Ma, Z.;Yang, X. (2019). Fundamentals of TiO2 Photocatalysis: Concepts, Mechanisms, and Challenges. *Advanced Materials*. *50* (31), 1901997.

[14] Mansouri, G.;Mansouri, M. (2020). Photocatalytic activity investigation of ZnO-TiO2 stabilized on ZSM-5 zeolite for Methyl Orange degradation. *Applied Chemistry Today*. *56* (15), 241-256.

[15] Samiee Paghaleh, E.;Kolvari, E. (2023). Green and Environmentally Sustainable Fabrication of CuFe2O4/CuO-rGO@EosinY as Photocatalyst for the Synthesis of Xanthene Derivatives. *Applied Chemistry Today*. *69* (18), 85-100.

[16] Franchi, D.;Amara, Z. (2020). Applications of Sensitized Semiconductors as Heterogeneous Visible-Light Photocatalysts in Organic Synthesis. *ACS Sustainable Chemistry & Engineering*. *41* (8), 15405-15429.

[17] Humayun, M.;Raziq, F.;Khan, A.;Luo, W. (2018). Modification strategies of TiO2 for potential applications in photocatalysis: a critical review. *Green Chemistry Letters and Reviews*. *2* (11), 86-102.

[18] Watanabe, M. (2017). Dye-sensitized photocatalyst for effective water splitting catalyst. *Science and Technology of Advanced Materials*. *1* (18), 705-723.

[19] Dianat, S.;Saranjam, N. (2025 .(Photocatalytic Degradation of Direct Red 23 and Direct Brown 166 Azo Dyes Using Polyoxometalate-Titanium Dioxide Nanocomposite. *Applied Chemistry Today*. *74* (20), 41-68.

[20] Gonuguntla, S.;Kamesh, R.;Pal, U.;Chatterjee, D. (2023). Dye sensitization of TiO2 relevant to photocatalytic hydrogen generation: Current research trends and prospects. *Journal of Photochemistry and Photobiology C: Photochemistry Reviews*. (57), 100621.

[21] Akhtaruzzaman, M.;Shahiduzzaman, M.;Selvanathan, V.;Sopian, K.;Hossain, M.I.;Amin, N.;Hasan, A.K.M. (2021). Enhancing spectral response towards high-performance dye-sensitised solar cells by multiple dye approach: A comprehensive review. *Applied Materials Today*. (25), 101204.

[22] Huang, J.-F.;Lei, Y.;Luo, T.;Liu, J.-M. (2020 .(Photocatalytic H2 Production from Water by Metal-free Dye-sensitized TiO2 Semiconductors: The Role and Development Process of Organic Sensitizers. *ChemSusChem*. *22* (13), 5863-5895.

[23] Richhariya, G.;Kumar, A.;Tekasakul, P.;Gupta, B. (2017). Natural dyes for dye sensitized solar cell: A review. *Renewable and Sustainable Energy Reviews*. (69), 705-718.

[24] Ludin, N.A.;Al-Alwani Mahmoud, A.M.;Bakar Mohamad, A.;Kadhum, A.A.H.;Sopian, K.;Abdul Karim, N.S. (2014). Review on the development of natural dye photosensitizer for dye-sensitized solar cells. *Renewable and Sustainable Energy Reviews*. (31), 386-396.

[25] Kushwaha, R.;Srivastava, P.;Bahadur, L. (2013). Natural Pigments from Plants Used as Sensitizers for TiO2 Based Dye-Sensitized Solar Cells. *Journal of Energy*. *1* (2013), 654953.

[26] Safie, N.E.;Ludin, N.A.;Su'ait, M.S.;Hamid, N.H.;Sepeai, S.;Ibrahim, M.A.;Teridi, M.A.M. (2015). Preliminary study of natural pigments photochemical properties of curcuma longa l. and lawsonia inermis l. as tio 2 photoelectrode sensitizer. *Malaysian Journal of Analytical Sciences*. *6* (19), 1243-1249.

[27] Amano, F.;Nakata, M.;Yamamoto, A.;Tanaka, T. (2016). Rutile titanium dioxide prepared by hydrogen reduction of Degussa P25 for highly efficient photocatalytic hydrogen evolution. *Catalysis Science & Technology*. *14* (6), 5693-5699.

[28] Li, X.;Shi, J.-L.;Hao, H.;Lang, X. (2018). Visible light-induced selective oxidation of alcohols with air by dye-sensitized TiO2 photocatalysis. *Appl Catal B*. (232), 260-267.

[29] Yang, X.;Zhao, H.;Feng, J.;Chen, Y.;Gao, S.;Cao, R. (2017). Visible-light-driven selective oxidation of alcohols using a dye-sensitized TiO2-polyoxometalate catalyst. *Journal of catalysis*. (351), 59-66.

[30] Kader, D.A.;Mohammed, S.J. (2023). Emerging developments in dye-sensitized metal oxide photocatalysis: exploring the design, mechanisms, and organic synthesis applications. *RSC advances*. *38* (13), 26484-26508.

[31] Marks, R.;Yang, T.;Westerhoff, P.;Doudrick, K. (2016). Comparative analysis of the photocatalytic reduction of drinking water oxoanions using titanium dioxide. *Water research*. (104), 11-19.

[32] Li, Y.;Wasgestian, F. (1998). Photocatalytic reduction of nitrate ions on TiO2 by oxalic acid. *Journal of Photochemistry and Photobiology C: Photochemistry Reviews*. *2-3* (112), 255-259.

[33] Yang, T.;Doudrick, K.;Westerhoff, P. (2013). Photocatalytic reduction of nitrate using titanium dioxide for regeneration of ion exchange brine. *Water research*. *3* (47), 1299-1307.